17. Hougen, O. A., and K. M. Watson, *Ind. Eng. Chem.*, **35**, 529 (1943).
18. Iwasaki, Takahisa, and Rikijiro Hatta, *Kogyo Kagaku Zasshi*, **63**, 1975-1979 (1960).
19. *Ibid.*, 1980-1985.
20. Johanson, L. N., and K. M. Watson, *Natl. Petrol. News, Tech. Sec.*, **38**, No. 32, 629 (1946).
21. Kemp, J. D., *U. S. Pat. 2,527,824* (1950).
22. Langlois, G. E., *U. S. Pat. 2,585,899* (1952).
23. Luzar, R. V., M.S. thesis, Pennsylvania State Univ. (1961).
24. McCaulay, D. A., and A. P. Lien, *J. Am. Chem. Soc.*, **74**, 6246-6250 (1952).
25. Octafining (Anon.), *Hydrocarbon Processing Petrol. Refiner*, **42**, 206 (Nov., 1963).
26. Pfennig, Reuben, *U. S. Pat. 2,632,779* (1953).
27. Pitts, P. M., Jr., J. E. Conner, Jr., and L. N. Leum, *Ind. Eng. Chem.*, **47**, 770-773 (1955).
28. Schnurmann, Robert, and Edward Kendrick, *Anal. Chem.*, **26**, 1263 (1954).
29. Schrieshiem, Alan, *J. Org. Chem.*, **26**, 3530-3533 (1961).
30. Takita, Kinichi, *Japan. Pat. 17,227.*
31. Taylor, W. J., et al., *J. Res. Natl. Bur. Standards*, **37**, 95-118 (1946).
32. Tsutsumi, Shigeru, and Masanobu Nakamura, *Technol. Rept. Osaka Univ.*, **10**, 509-513 (1960).
33. Satterfield, C. N., and T. K. Sherwood, "The Role of Diffusion in Catalysis," Addison-Wesley, Reading, Mass. (1963).

Manuscript received October 25, 1965; revision received July 25, 1965; paper accepted July 25, 1965. Paper presented at A.I.Ch.E. Minneapolis meeting.

Electrokinetic-Potential Fluctuations Produced by Pipe Flow Turbulence

HSING CHUANG and J. E. CERMAK

Colorado State University, Fort Collins, Colorado

The distribution across a pipe of turbulent intensities, shearing stress, and energy spectra are inferred from measured electrokinetic-potential fluctuations in a fully developed flow of distilled water in a 2.54-cm. diameter glass pipe. These quantities are shown to be in good agreement with those obtained by Laufer and Sandborn with hot-wire anemometers for air flows at the same mean Reynolds number. A tentative analytical model of the phenomenon is constructed and analyzed by Maxwell's electrodynamic field equations for a nonmagnetized medium moving with a velocity which is much smaller than the velocity of light. A set of equations governing the interrelation between the electrokinetic-potential fluctuations and the turbulent velocity-fluctuation components of the flow field in fully developed pipe flow is deduced. Fourier transforms are then introduced and simple relations between the electrokinetic-potential fluctuations and velocity fluctuations are obtained.

The electrokinetic phenomenon was first observed early in the 19th century. The basic idea of an electrical double layer or diffused double layer arising from adsorption of fluids in contact with solid walls was formed and developed during the last hundred years. The fundamental formulation of the electrokinetic phenomenon is attributed to Helmholtz. However, all early experiments and theories of the electrical double layer were concerned with either a laminar flow through a small tube or a flow through a porous diaphragm connecting two liquid containers. Only recently has the study of electrokinetics been extended to turbulent shear flow.

The instantaneous fluctuations of the streaming potential which occur in a turbulent flow were first observed and recorded by Bocquet (*1*). Binder (*2*) was the first researcher to use electrokinetic measurements to infer velocity fluctuations near the wall in a turbulent fluid. Chuang used it to infer velocity fluctuations in a fully developed pipe flow (*3*) and an open channel flow (*4*).

Because of the many experimental difficulties which arise, it is impossible to explore the characteristics of turbulent motion very close to a wall with existing techniques. Our present knowledge of turbulent shear flow in close proximity to a wall is still insufficient to be the basis for a sound and complete theory. It was this particular problem which motivated this study of electrokinetics in a turbulent flow of distilled water.

Hsing Chuang is at the University of Louisville, Louisville, Kentucky.

EXPERIMENTAL EQUIPMENT AND PROCEDURE

The experimental equipment consists of the flow system, the electrodes, and the electrical measurement equipment. The flow system is a self-circulating facility as shown in Figure 2. It has a constant-head tank, 15 cm. in diameter, which provides a constant head of 360 cm., upstream and down-

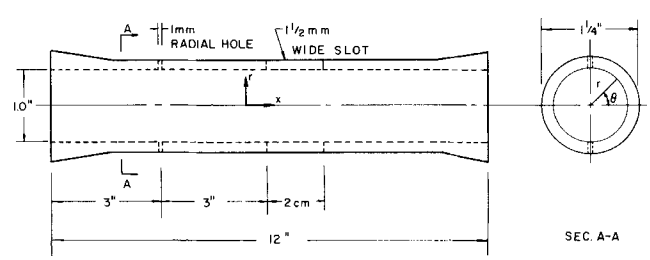

Fig. 1. Test section.

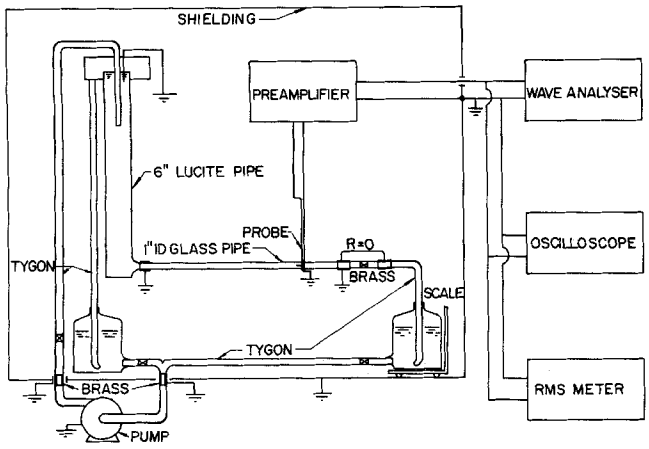

Fig. 2. Flow system and electrical measurement equipment.

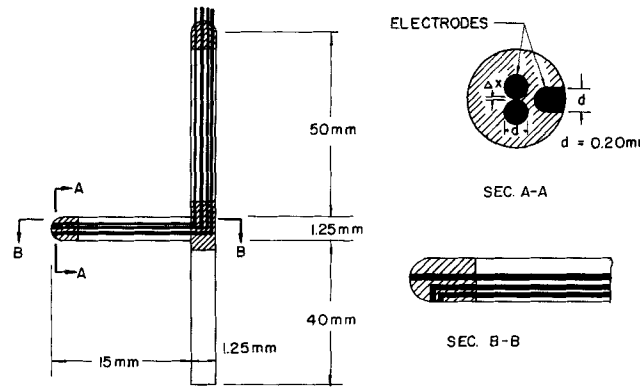

Fig. 4. Probes.

stream reservoirs, a stainless steel pump driven by a ½-h.p. electric motor, and a circular glass pipe about 520 cm. long. These components are interconnected by Tygon tubing and are made of relatively inert materials. The circular pipe consists of nine pieces of glass and Lucite pipes of various lengths, all 2.54 cm. I.D. The pipe sections are connected by precision couplings. The test section, which is shown in Figure 1, can thus be inserted at various axial positions. The flow rate in the pipe was regulated by the valves located at the downstream end of the pipe and was stabilized by regulating the outflow from each reservoir. Equilibrium water with a conductivity of about 5×10^4 mhos/m. at 20°C. was used as the fluid throughout this work.

The electrodes are made of magneto wire (that is, varnished, commercial grade copper) of 0.16 and 0.20 mm. in diameter, and are supported by a probe of stainless steel tubing. As shown in Figures 3 and 4, three kinds of probes were used. The cylindrical probe is made by drilling a hole on the tube wall, inserting two insulated magneto wires into the tube through the hole, and then gluing them to the tube with an epoxy cement. The electrodes are fastened closely and aligned in such a manner that when the probe moves up and down in the radial direction, the electrodes are in the circumferential direction. The same method of construction was used to make the T-shaped probes but different sizes of the magneto wire and external tubing were used. This type of electrode alignment was used to measure the circumferential electrokinetic-potential fluctuations due to the velocity fluctuation in this direction. The probes for the measurement of electrokinetic-potential fluctuations due to the turbulent shearing stress and the turbulent velocity fluctuations in both the axial and the radial directions have four electrodes, two electrodes for each direction, fastened closely and aligned in each direction. The probe was inserted into the pipe through a slot in the test section and was connected to a micrometer supported by a rigid frame. Experimental evidence revealed no quantitative difference in the measured signals due to the difference in wire size (0.16 and 0.20 mm.) or to the difference in external tube size (0.80 and 1.25 mm.).

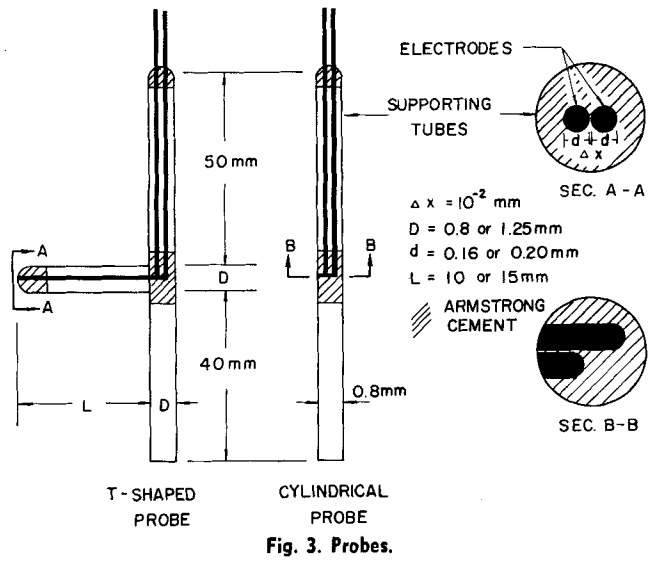

Fig. 3. Probes.

The electrical measurement equipment is shown in Figures 2 and 5. The equipment shown in Figure 2 was used for the measurement of the distribution and the spectral density function of the turbulent intensities across the pipe, while that shown in Figure 5 was used for the measurement of the spatial distribution and spectral density distribution of the shearing stress across the pipe. The low-level differential preamplifier (Tektronix type 122) was used to amplify the signal. This amplifier has selective gain and frequency response ranges which were set at 1,000 × and from 0.2 to 10,000 cycles/sec., respectively, throughout the measurements. The output of the preamplifier was then fed into either a wave analyzer (Hewlett-Packard model 300A), or an RMS meter (Hewlett-Packard model 400H), or an oscilloscope (Tektronix type 502). The wave analyzer with a frequency response range from 20 to 16,000 cycles/sec. has a narrow band pass of less than 10 cycles/sec. at the half-power point. However, at frequencies near zero, the wave analyzer's selectivity is not well defined so that the spectral data were taken only at frequencies above 30 cycles/sec. The RMS meter has a voltage range from 0.1 mv. to 300 v. and a frequency-response range from 10 to 4×10^6 cycles/sec. The oscilloscope was used to view the randomness of the potential fluctuations and for detecting any anomaly such as spikes or 60-cycle pickup. The impedance between the electrodes through the liquid, in parallel with the input impedance of the preamplifier of about 10^7 ohms, was computed to be about 10^5 ohms. The time constant was estimated to be about 5×10^{-6} sec., which was smaller than the period of the highest frequency to be passed by the preamplifier; that is, 10^{-4} sec., so that the amplifying circuit was appropriate. A true root-mean-square

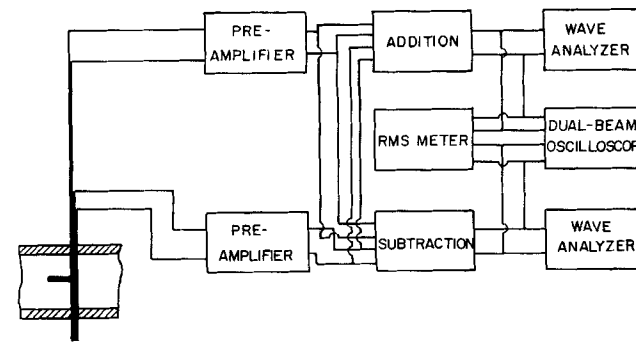

Fig. 5. Electrical measurement equipment for turbulent shearing stress measurement.

analyzer (Hubbard Instrument Model L) with adding and subtracting channels was used for the instantaneous signal addition and subtraction. The external probe tubing and some other points of the system were grounded as shown in Figure 2. After the completion of the research reported here, it was found that a.c. power sources inside the shielded cage did not affect the electrokinetic signals. However all the data presented herein were taken without a.c. power within the cage. The overall noise was measured before each run and the corresponding readings were corrected for the noise (3).

The usual experimental procedure consisted of an electronic instruments warm-up period and a calibration before and during the data acquisition. Therefore, there should be little systematic error in the data due to instrument drift. The flow rate which could be changed by regulating the downstream valve was determined at the beginning of each run. Some electrokinetic measurements were made at two sections of the pipe about 290 and 411 cm. from the pipe entrance. These data exhibited no systematic difference, which implied that the flow was fully developed. Subsequently, measurements were made only at the downstream section.

DISCUSSION OF EXPERIMENTAL RESULTS

The fluctuation of electrokinetic potential difference between two closely spaced electrodes aligned in any direction is considered to be linearly proportional to the fluctuating turbulent velocity in that direction. This assumption is based on the analysis (3) that the thickness of the double layer formed on the solid-liquid interfaces is about 10^{-5} cm. and that the fluctuation of turbulent velocity carries along with it the time-mean charge density. The resulting effect is a local gradient of the electrokinetic potential which is sensed by the electrodes. The electrokinetic probes were not calibrated so that only the functional forms of the various turbulent intensities could be obtained.*

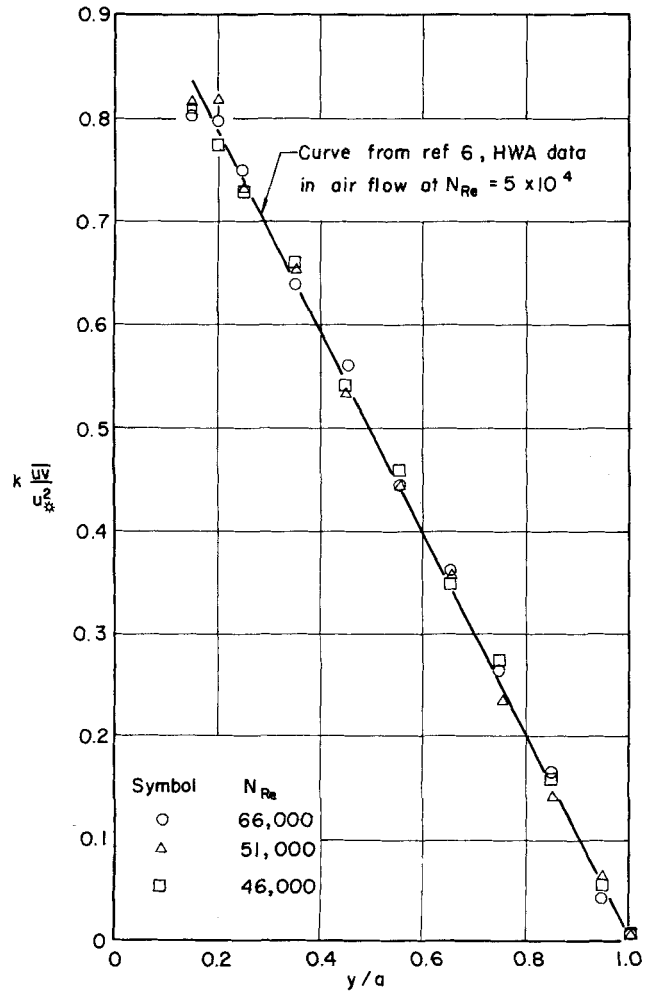

Fig. 6. Turbulent shearing stress distribution.

Turbulent Shearing Stress Distribution

The turbulent shearing stress was deduced from the measured electrokinetic-potential difference fluctuation at y/a = 0.15, 0.20, 0.25, 0.35, 0.45, 0.55, 0.65, 0.75, 0.85, 0.95, and 1.00 (center of the pipe) for Reynolds numbers 66,000, 51,000, 46,000, 31,000, and 17,000. The results are shown in Figure 6 where K is an arbitrary constant. The solid line represents Pai's equation (5) with the arbitrary constants n and s determined from Laufer's experimental data (6) at Reynolds number 5×10^4. The results for Reynolds numbers of 31,000 and 17,000 were discarded because of low signal-to-noise ratio of the electrokinetic measurements at these runs.

Turbulent Intensity Correlations

The turbulent intensities inferred from the electrokinetic potential data, which were taken at those points mentioned in the previous paragraph for the same Reynolds numbers, are shown in Figures 7, 8, and 9, where a local isotropy at the center of the pipe was assumed (7) for the highest Reynolds number, 66,000. All inferred turbulent intensities decrease with the Reynolds number. Again the results for Reynolds numbers 31,000 and 17,000 were discarded for the same reason mentioned before. For comparison, the functional forms of Laufer's experimental data were also plotted in these figures. The electrokinetic data show good agreement with Laufer's results for the same Reynolds number. It also shows that the degree of anisotropy of turbulence increases toward the pipe wall in every case.

The double-correlation coefficient was computed from the inferred turbulent shearing stress and intensity data. The result is shown in Figure 10. Again good agreement with Laufer's anemometer data is revealed for the same Reynolds number. The double-correlation coefficients deduced from Sandborn's experimental data (7) were also plotted in the figure. They show even better agreement with present results.

The relative values of turbulent intensities were plotted in Figures 11 and 12. As mentioned before, a local isotropy at the center of the pipe was assumed to force v'/u' and w'/u' to unity at this point for the highest Reynolds number. This assumption is not necessarily true for low Reynolds numbers such as those considered in this experiment. The degree of anisotropy is thus shown more clearly to increase toward the pipe wall. These data also indicate the degree of anisotropy of the turbulent intensities of the radial and the circumferential components toward the wall. All data for Reynolds numbers around 5×10^4 show good agreement with Laufer's experimental data obtained by using hot-wire anemometers in air flows. The relative values of turbulent intensities calculated from Sandborn's experimental data are also shown. The anisotropy at the center of the pipe is more pronounced for these data.

Spectra of E_u, E_v, E_w, and E_{uv}

Spectral distributions of the electrokinetic-potential fluctuations in every direction show continuous increase with Reynolds number. This trend is consistent with the assumed interrelation between the electrokinetic-po-

* No direct calibration technique for the probe is yet available. It is rather difficult to devise an absolute calibration of the probe.

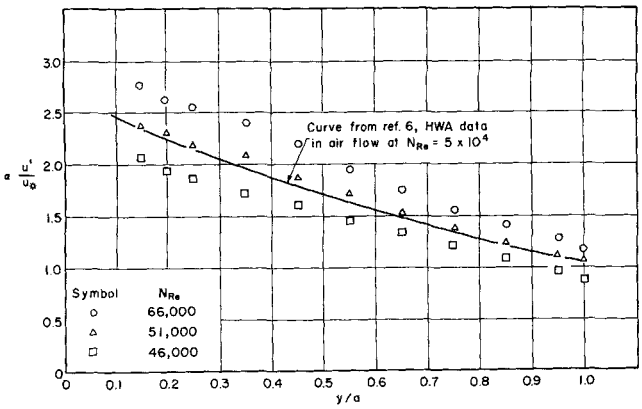

Fig. 7. Turbulent intensity of u' across the pipe.

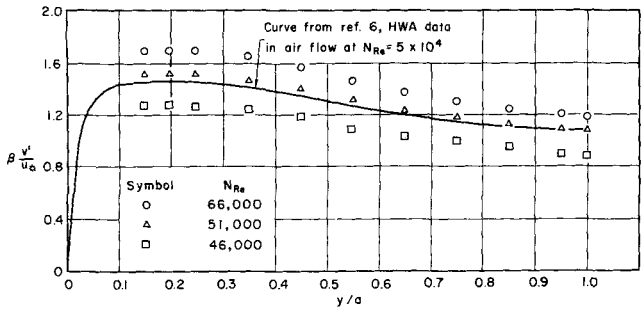

Fig. 8. Turbulent intensity of v' across the pipe.

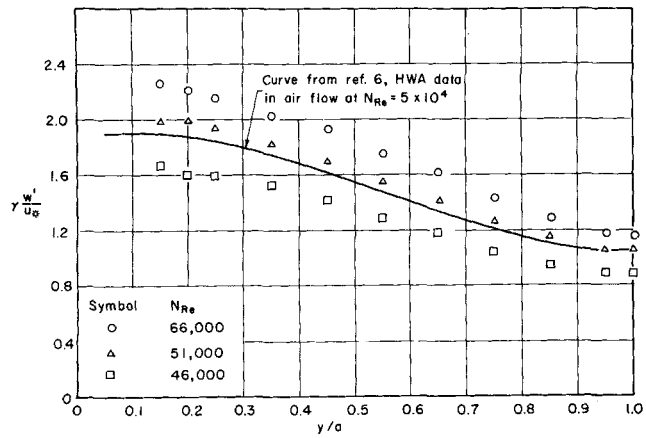

Fig. 9. Turbulent intensity of w' across the pipe.

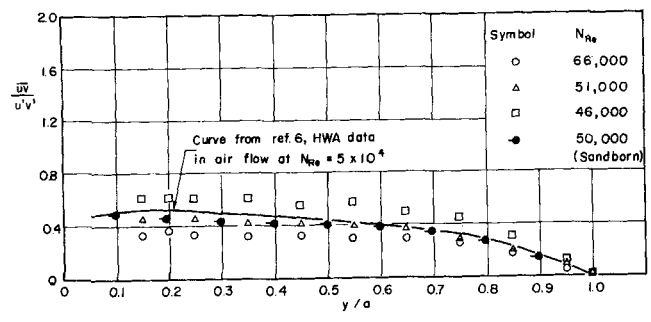

Fig. 10. Double-correlation coefficient distribution.

tential fluctuations and the turbulent velocity fluctuations, because the intensity of turbulence of the flow field increases with Reynolds number as shown experimentally by Sandborn (7). The inferred spectral distributions of turbulent energy and shearing stress are shown in Figures 13 to 16, which are now examined to gain further insight into the turbulent shear flow. Theoretical analysis of the energy spectrum in nonisotropic homogeneous turbulence with a uniform mean flow is summarized by Hinze (8). However, because of the complexity of the problem near a solid boundary where mean turbulent shearing stresses are present, no theory on the turbulent energy spectrum in nonisotropic wall turbulence has yet been developed. Nevertheless, electrokinetic measurements of the spectral distributions of turbulent energy and shearing stress in this type of flow may be of assistance in studying the turbulent shear flow.

The mechanism of turbulent shear flow consists of production, diffusion, transfer, convection, and dissipation of turbulent energy. In general, the effects of the diffusion and convection of turbulent energy are assumed to be confined to the very low wave numbers which lie outside the equilibrium range and are negligible in the wave number range measured in this experiment. By assuming that the production of turbulent energy predominates in the low wave number region or large eddies, Tchen (9) predicted a spectral distribution varying as n^{-1} for this region. This low wave number region is generally observed only in the spectra of the turbulent velocity component in the direction of the main flow in low-speed air flows. The transfer region is characterized by a spectral variation of $n^{-5/3}$ and this region exists over a wide wave number range where the turbulent energy is transferred from the larger eddies to the smaller eddies through the spectrum without being significantly influenced by the turbulent energy production or dissipation mechanisms. This concept is limited to large turbulent Reynolds numbers and it has received some experimental support from Laufer (6). For the higher wave number range, the viscous dissipation mechanism predominates and the spectral variation is n^{-7}. However, experimental data by many researchers indicate a continuously increasing slope exceeding the negative power of 7.

The inferred E_u spectra, as shown in Figure 13, have only limited ranges of the -1 and $-5/3$ powers of the wave number n. However, these curves vary as a $-7/2$ power of n over a considerable range. This phenomenon might indicate some characteristics of the nonisotropic turbulent shear flow at low Reynolds numbers. The functional forms of the experimental data taken by Sandborn at the pipe center, for Reynolds number 5×10^4 were also plotted and good agreement was revealed. The -1 power of n is absent in E_v and E_w spectra shown in Figures 14 and 15, respectively. The $-5/3$ and $-7/2$ powers of n are indicated to take place over considerable ranges for flows at Reynolds number 51,000. However, for flows at lower Reynolds number, only the $-5/2$ power of n occurs over an appreciable range. These phenomena might also disclose a characteristic of the flow at low Reynolds number. The spectra of E_v and E_w are significantly different from those of E_u in the smaller wave number region and the absence of -1 power of n in these spectra has thus confirmed the prediction by Tchen (9).

Spectral distribution of the turbulent shearing stress is shown in Figure 16. These spectra are valuable for a direct test of local isotropy as discussed by Klebanoff (10). The present experimental data indicate that no local isotropy has been attained when compared with the results of reference 10.

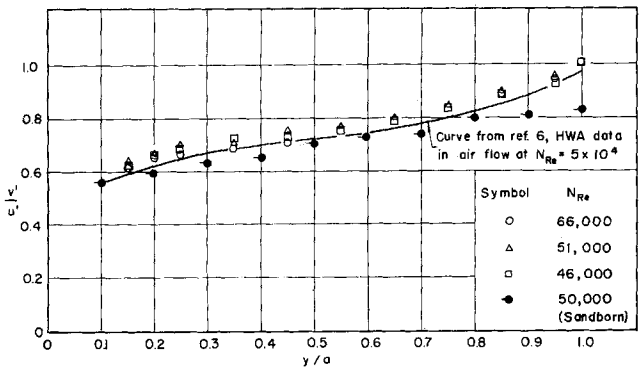

Fig. 11. Distribution of v'/u' across the pipe.

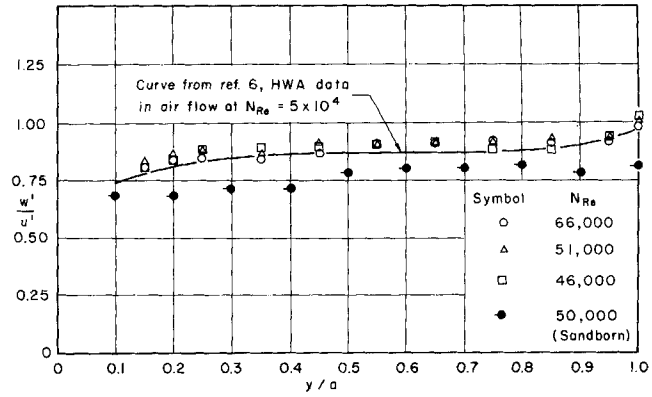

Fig. 12. Distribution of w'/u' across the pipe.

TENTATIVE THEORY

Fully developed turbulent motion of an incompressible fluid flowing in a pipe of circular cross section will be studied. It has the property of homogeneity in both the longitudinal and the circumferential directions; thus all Eulerian time-mean values at a given point are functions of r, the radial coordinate only.

In turbulent motion both scalar and vector quantities exhibit random fluctuations, and generally, some correlations should exist among them. As discussed by Binder (2), electrokinetic-potential fluctuations are generated whenever the true charge density is transported in the turbulent flow field. It is therefore a general objective of this analysis to find some correlation between the electrokinetic-potential fluctuations and the velocity fluctuation components.

Maxwell's electrodynamic field equations (*11*) for a nonmagnetized medium moving with a velocity **U**, which is small compared to the velocity of light, together with the generalized Ohm's law and the equation of mass conservation for an incompressible fluid, yield the equation of continuity for electrodynamics in moving medium. After some mathematical manipulation and simplification, this relation may be written as (3)

$$\frac{\partial \rho}{\partial t} + (\mathbf{U} \cdot \nabla)\,\rho + \frac{\rho}{\tau} = 0 \qquad (1)$$

The relaxation time τ is a characteristic time of the fluid and represents the time necessary for restoration of the original equilibrium charge distribution after the initiation of a disturbance.

Equation (1) shows that the sum of the material derivative of true charge density and the change of true charge density during the time τ is equal to zero. By separating the turbulent quantities in Equation (1) into a time-mean quantity and a fluctuating quantity, one has

$$\frac{\partial \rho_t}{\partial t} + \nabla \cdot [(\bar{\rho} + \rho_t)(\bar{\mathbf{U}} + \mathbf{u})] + \frac{1}{\tau}(\bar{\rho} + \rho_t) = 0$$

Taking the time averages of the above equation and then subtracting these time averaged quantities from the above equation, one gets

$$\frac{\partial \rho_t}{\partial t} + \nabla \cdot [\bar{\rho}\mathbf{u} + \rho_t(\bar{\mathbf{U}} + \mathbf{u}) - \overline{\rho_t \mathbf{u}}] + \frac{1}{\tau}\rho_t = 0 \qquad (2)$$

Equation (2) is the equation of continuity, in electrodynamics, for the fluctuating and time mean components of ρ and **U** in a moving medium.

By introducing the vector and scalar potentials and the Lorentz condition into Maxwell's electrodynamic field equations, it is possible to derive a set of inhomogeneous wave equations. As before, by separating the instantaneous quantities into mean and fluctuating quantities, and by subtracting from the instantaneous wave equation its time averages, one obtains the fundamental differential equation for the potential fluctuations about its mean value as follows (3):

$$\nabla^2\psi - \mu\epsilon\kappa\frac{\partial^2\psi}{\partial t^2} - \mu\sigma\frac{\partial\psi}{\partial t} = -\frac{\rho_t}{\kappa\epsilon} \qquad (3)$$

Equation (3) requires some further explanation. If the fluid is a good conductor, the second term on the left side will drop out, whereas if the fluid is a good dielectric, the third term on the left side will drop out. Equation (3)

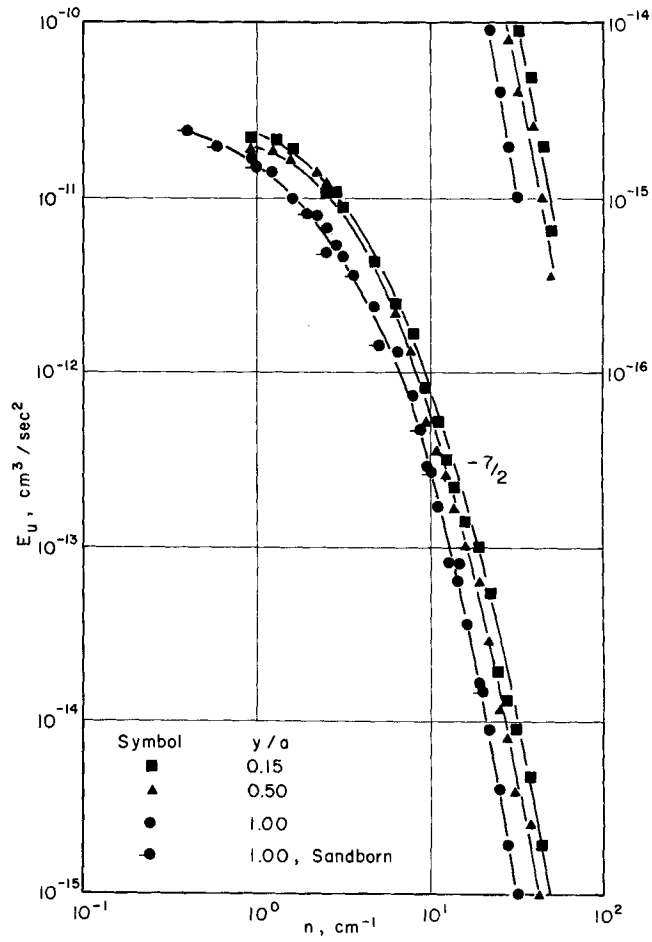

Fig. 13. Spectra of E_u, N_{Re} = 51,000.

in conjunction with Equation (2) and the assumption that $\tau \overline{U}_{max} n_{max} << 1$, gives the following simple relation

$$\nabla^2 \psi = \frac{1}{\sigma} \nabla \cdot (\bar{\rho} \mathbf{u}) \tag{4}$$

Since it is implicit in the foregoing analysis that the fluid is homogeneous in the pipe, the bulk conductivity of the fluid is constant. The thickness of the double layer formed on the solid-liquid interfaces is small, about 10^{-5} cm. The previous equation can be rewritten as

$$\nabla \cdot (\sigma \nabla \psi - \bar{\rho} \mathbf{u}) = 0$$

or

$$\nabla \cdot (\sigma \mathbf{e} - \mathbf{j}) = 0$$

The fluctuating field intensity or the induced a.c. field intensity is fluctuating about the induced d.c. field intensity. The fluctuating current density is generated through the transport of the mean true charge density by the turbulent velocity-fluctuation components. The first term in the parenthesis, according to Ohm's law, is also a fluctuating current density due to the induced a.c. field intensity. Thus, the above equation shows a conservation of fluctuating current density in the elemental control volume of fluid.

Let the difference of the fluctuating current densities in each direction be Δj_x, Δj_r, and Δj_θ, respectively. The above equation can then yield

$$\frac{\partial}{\partial x}(\Delta j_x) + \frac{1}{r}\frac{\partial}{\partial r}(r \Delta j_r) + \frac{1}{r}\frac{\partial}{\partial \theta}(\Delta j_\theta) = 0$$

Equation (4) and the above equation are in fact identical. Consequently, they give

$$\sigma \frac{\partial \psi}{\partial x} - \bar{\rho} u = \Delta j_x$$

$$\sigma \frac{\partial \psi}{\partial r} - \bar{\rho} v = \Delta j_r \tag{5}$$

and

$$\frac{\sigma}{r}\frac{\partial \psi}{\partial \theta} - \bar{\rho} w = \Delta j_\theta$$

It is assumed that Δj_x, Δj_r, and Δj_θ are much smaller than the fluctuating current densities due to the fluctuating velocity components and the fluctuating current densities in terms of the induced potential fluctuation gradients. In other words, as a first approximation, the fluctuating current densities due to the turbulent flow may be considered to be almost counterbalanced in each direction by the corresponding induced potential fluctuation gradients.

Equation (5) constitutes the proposed differential equations for electrokinetic-potential fluctuations. They reveal that the main cause of the electrokinetic-potential fluctuations may be the transport of the mean true charge density by the corresponding velocity-fluctuation component.

By introducing Fourier transforms and substituting a potential-difference fluctuation between two closely spaced electrodes in lieu of the potential-fluctuation component, Chuang (3) has derived the following equations from the set labeled Equation (5):

$$E_u(n) = K_1 \quad E_{\Delta\psi x}(n)$$

$$E_v(n) = K_2 \quad E_{\Delta\psi r}(n)$$

$$E_w(n) = K_3 \quad E_{\Delta\psi\theta}(n) \tag{6}$$

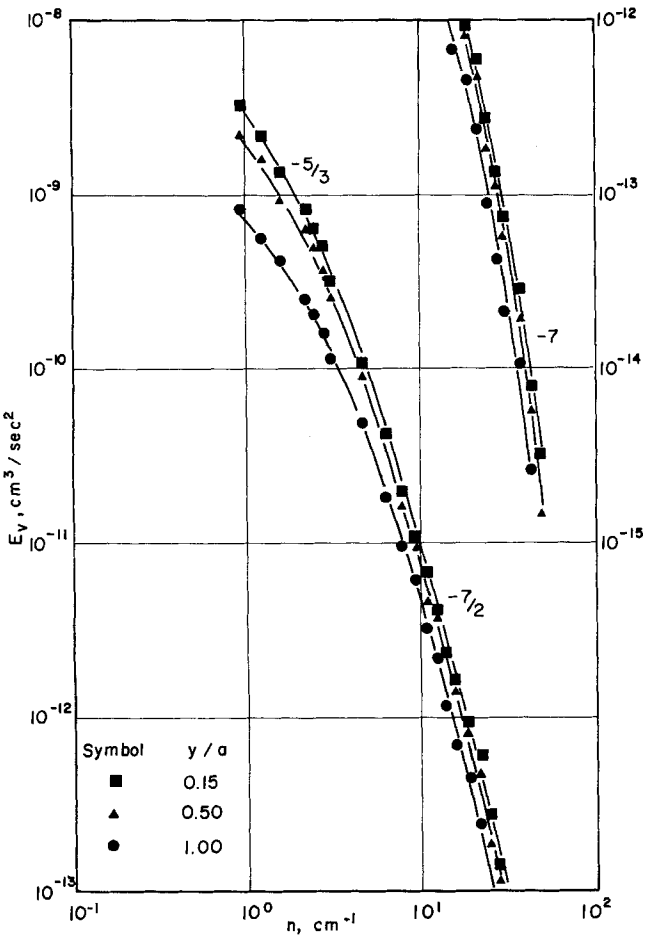

Fig. 14. Spectra of E_v, N_{Re} = 51,000.

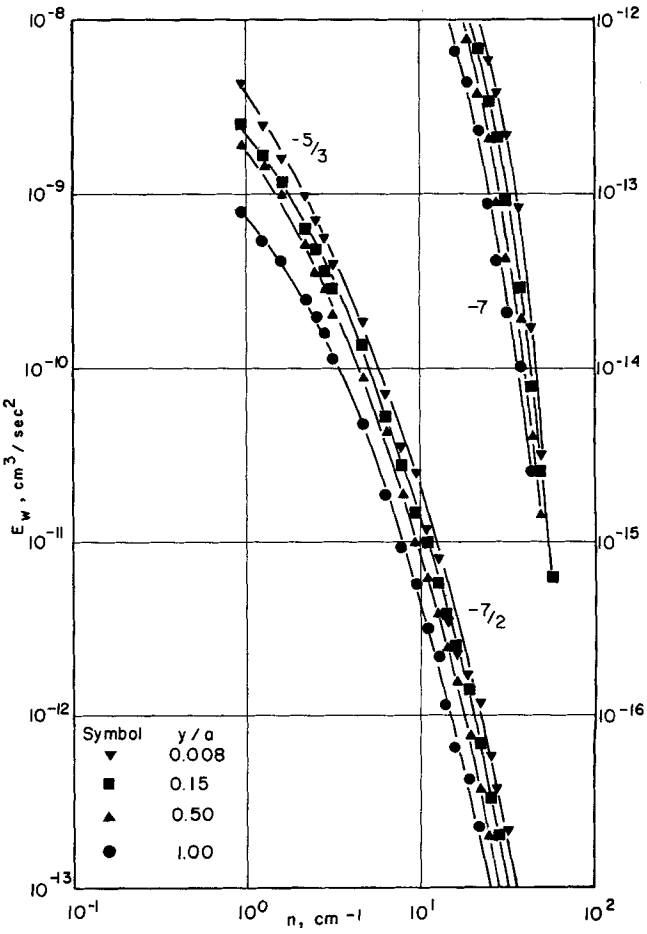

Fig. 15. Spectra of E_w, N_{Re} = 51,000.

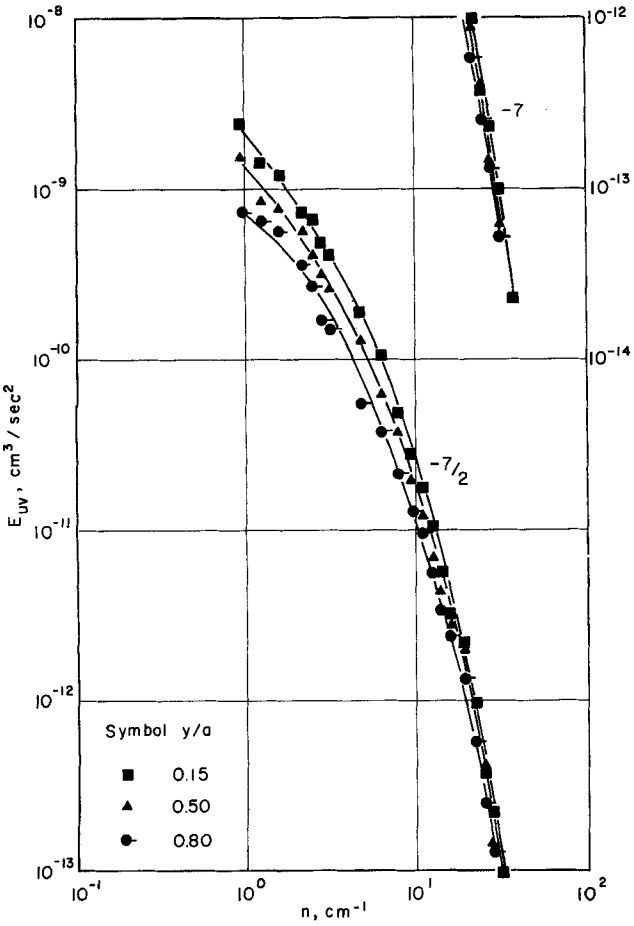

Fig. 16. Spectra of E_{uv}, N_{Re} = 51,000.

and

$$E_{uv}(n) = K_4 \quad E_{\Delta\psi xr}(n)$$

Equation (6) shows that for a homogeneous fluid at a constant temperature, the spectral distributions of turbulent energies and shearing stress are directly proportional to the corresponding energy spectral distributions of the electrokinetic-potential fluctuation difference.

An electrical double layer is presumed to exist at the solid-liquid interface between the probe, which contains the closely spaced electrodes, and the water. However, the thickness of the double layer is extremely small compared to the size of the probe.

CONCLUSIONS

1. The electrokinetic-potential fluctuations at any point in the flow field of fully developed pipe flow of distilled water are measurable by means of the electrokinetic probe.
2. The inferred turbulent intensities and shearing stress are in good agreement with Laufer and Sandborn's hot-wire anemometer data for air flow through a pipe at the same mean Reynolds number.
3. The inferred energy spectra indicate some characteristics of the turbulent shear flow at low Reynolds number and are in good agreement with Sandborn's anemometer data for $N_{Re} = 5 \times 10^4$ in air flow.
4. The assumed relation between the electrokinetic-potential fluctuations and the turbulent velocity fluctuations given by Equations (5) and (6) are supported by the experiment.
5. The technique of electrokinetic-potential fluctuation measurements may be valuable for research on turbulence in fluids. However, an absolute calibration technique must be devised before it can meet the requirements as a turbulence transducer.

ACKNOWLEDGMENT

Valuable discussion with Dr. L. V. Baldwin is sincerely appreciated. Financial support for this study was provided by the National Science Foundation through Grant 10176.

NOTATION

D = pipe diameter, cm.
E_i = turbulent energy in the i direction associated with the wave number dn, cc./sec.^{2}
$E_{\Delta\psi i}$ = electrokinetic-potential difference in the i direction associated with the wave number dn, v.^{2}—cm.
$\mathbf{e}$ = induced a.c. field intensity, v./cm.
$\mathbf{j}$ = fluctuating current density, amp./sq.cm.
K_i = arbitrary constant
N_{Re} = U_cD/ν, Reynolds number
n = wave number, cm.$^{-1}$
r = radial coordinate in cylindrical coordinates, cm.
t = time, sec.
$\mathbf{U}$ = velocity vector
$\overline{\mathbf{U}}$ = time mean velocity vector
U_c = maximum velocity at center of pipe, cm./sec.
$\mathbf{u}$ = fluctuating velocity vector
x = axial coordinate in cylindrical coordinates, cm.
∇ = differential operator

Greek Letters

α = arbitrary constant
β = arbitrary constant
γ = arbitrary constant
ϵ = electric constant
θ = circumferential coordinate in cylindrical coordinates, rad.
κ = dielectric constant
μ = absolute permeability
ν = kinematic viscosity, sq.cm./sec.
ρ = true charge density, coulomb/cc.
$\overline{\rho}$ = time-mean charge density, coulomb/cc.
ρ_t = fluctuating charge density, coulomb/cc.
σ = electrical conductivity of the medium, mho/cm.
τ = relaxation time of the medium, $\tau = \kappa\epsilon/\sigma$, sec.
ψ = fluctuating electrokinetic potential, v.

LITERATURE CITED

1. Bocquet, P. E., C. M. Sliepcevich, and D. F. Bohr, *Ind. Eng. Chem.*, **48**, 197 (1956).
2. Binder, G. J., Ph.D. thesis, Colorado State Univ., Fort Collins (1960).
3. Chuang, Hsing, Ph.D. thesis, Colorado State Univ., Fort Collins (1962).
4. ———, and J. E. Cermak, *J. Hyd. Div. Am. Soc. Civil Engrs.*, **91**, HY6 (1965).
5. Pai, S. I., *J. Franklin Inst.*, **256**, 337 (1953).
6. Laufer, John, *Natl. Advisory Comm. Aeronaut. Tech. Note 2954* (1953).
7. Sandborn, V. A., *ibid., 3266* (1955).
8. Hinze, J. O., "Turbulence," McGraw-Hill, New York (1959).
9. Tchen, C. M., *U.S. Natl. Bur. Std. Res. Paper RP 2388, J. Res.*, **50**, 51 (1953).
10. Klebanoff, P. S., *Natl. Advisory Comm. Aeronaut. Rept. 1247* (1955).
11. Panofsky, W. K., and M. Phillips, "Classical Electricity and Magnetism," Addison-Wesley, Mass. (1956).

Manuscript received January 27, 1965; revision received August 16, 1966; paper accepted August 16, 1966.